

## BOUNDARY-LAYER SEPARATION IN TWO-LAYER FLOW PAST A CYLINDER IN A ROTATING FRAME

**Michael A. Page**  
Department of Mathematics  
Monash University  
Clayton, Victoria  
Australia

**Peter Blanchonette**  
Air Operations Division  
AMRL-DSTO  
Melbourne, Victoria  
Australia

### ABSTRACT

This paper examines the motion of a two-layer viscous fluid past a circular cylinder relative to a rotating frame, under the Boussinesq approximation. Of particular interest is the motion in the boundary layers close to the cylinder in each layer, including the separation of these boundary layers from the surface.

### INTRODUCTION

The motion of a homogeneous fluid past an obstacle in a rotating frame has often been used as a prototype to examine the effect of Coriolis forces on large-scale geophysical flows past obstacles, such as isolated islands. This approach led to a series of experimental studies by Boyer and his colleagues (for example, Boyer 1970, Boyer & Davies 1982) which have identified some of the special features of this flow, one of which is a reduced tendency of the boundary layer to separate from the obstacle. While it could be argued that some of the features of these flows are different from those observed in the oceans, in particular the suppression of separation due to influence of the Ekman layers, it is nonetheless important to understand the origin of the features in the experiments and this had led to a series of theoretical and numerical studies of flow past obstacles in a rotating frame. Among these have been the studies by Barcilon (1970), Walker & Stewartson (1972), Merkin & Solan (1979), Matsuura & Yamagata (1986), Page (1987), Becker (1991) and Page & Duck (1993). All of these papers have concentrated on the influence that the thin viscous boundary layers on the surface of a circular cylindrical obstacle can have on the overall flow field as the Rossby number  $Ro$  is increased, particularly the suppression of separation for  $Ro \leq E^{1/2}$  when  $E \ll 1$ , where  $E$  is the Ekman number. Some disadvantages with this approach, which contribute to why it does not always model geophysical flows very effectively, are that the oceans and atmosphere are actually density stratified rather than homogeneous, and that their motion is

generally vertically sheared, rather than being constrained to be two dimensional as in a homogeneous rotating fluid. In practice, the additional effects due to these two properties can often overwhelm those due to the earth's rotation alone.

In this study, we extend the previous studies in a homogeneous fluid by considering the flow past obstacles in a two-layer fluid, which is a common prototype in theoretical studies on the effects of both density stratification and vertical shear in the flow (see, for example, Gill 1982). A similar study was performed by Brevdo & Merkin (1985), who examined the flow for zero Froude number  $F$  by calculating numerical solutions of the boundary-layer equations, under the assumption that the flow was not separated. Such an approach would be acceptable if the aim was to examine only the unseparated flow, but otherwise it fails due to the distortion of the outer potential-flow solution by the separated boundary layer. A better approach to the problem would be to follow that used by Page (1987) for the homogeneous rotating flow, which was based on Smith's (1985) study of the corresponding non-rotating problem, where the form of the *separated* potential flow is sought. However, it turns out that there is no simple way to extend that technique to a two-layer fluid, and so this paper uses some of the numerical calculations by Blanchonette (1995) for  $F = 0$  to re-examine some of Brevdo & Merkin's conclusions.

### THE GOVERNING EQUATIONS

Consider two layers of viscous fluid, of densities  $\rho_1^*$ ,  $\rho_2^*$  and kinematic viscosities  $\nu_1^*$ ,  $\nu_2^*$ , which have uniform velocities  $U_1^*$ ,  $U_2^*$  and depths  $d_1^*$ ,  $d_2^*$  far from a cylinder of radius  $l^*$ , as shown in Figure 1. The fluid is contained between two plates which are a distance  $d^* = d_1^* + d_2^*$  apart and the entire configuration rotating with a uniform angular velocity  $\Omega^*$  about an axis aligned with the cylinder. For a Boussinesq fluid the densities in each layer  $\rho_1^*$  and  $\rho_2^*$  are taken to be approximately equal,



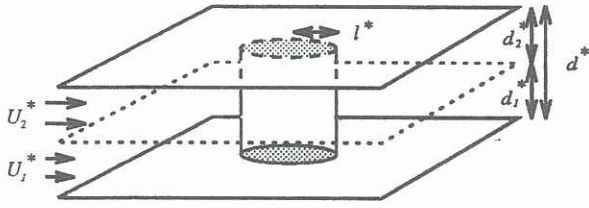


Figure 1 The two-layer flow configuration

with  $\Delta\rho^* = (\rho_1^* - \rho_2^*) > 0$  due to stability considerations, and for simplicity we assume in this paper that  $v_1^* = v_2^*$  and  $d_1^* = d_2^*$ , although these are not crucial to the analysis or form of the results.

Scaling all velocities by the average far-field velocity  $U^* = \frac{1}{2}(U_1^* + U_2^*)$ , all lengths by the cylinder radius  $l^*$ , and time by the inverse rotation rate  $1/\Omega^*$  we can define three non-dimensional dynamical parameters

$$Ro = U^*/\Omega^* l^* \quad (\text{Rossby number})$$

$$E = \nu^*/\Omega^* d^{*2} \quad (\text{Ekman number})$$

$$F = 4\rho_1^* \Omega^{*2} l^{*2} / g^* \Delta\rho^* d^* \quad (\text{Froude number})$$

with geometrical parameters  $d = d^*/l^*$  and  $d_1 = d_2 = d/2$ . As for the one-layer flow in Page (1987), we assume here that  $Ro$  and  $E$  are both small, and in particular that  $Ro$  is  $O(E^{1/2})$  for  $E \ll 1$  and that  $F$  is  $O(1)$ . Under these conditions it is appropriate to introduce the two scaled nondimensional parameters

$$\lambda = Ro/2E^{1/2} \quad \text{and} \quad \delta = d(\frac{1}{2}E^{1/2})^{1/2} \ll 1$$

which measure the relative size of nonlinear effects in comparison to Ekman-layer suction effects, and the scale thickness of the boundary layer, respectively. In terms of these parameters, the equations governing the flow are

$$\frac{\partial \Gamma_1}{\partial t} + \lambda(u_1 \frac{\partial \Gamma_1}{\partial x} + v_1 \frac{\partial \Gamma_1}{\partial y}) = \frac{1}{2}(\zeta_2 - 3\zeta_1) + \delta^2 \nabla_h^2 \zeta_1$$

and

$$\frac{\partial \Gamma_2}{\partial t} + \lambda(u_2 \frac{\partial \Gamma_2}{\partial x} + v_2 \frac{\partial \Gamma_2}{\partial y}) = \frac{1}{2}(\zeta_1 - 3\zeta_2) + \delta^2 \nabla_h^2 \zeta_2$$

(Blanchonette, 1995), where  $t$  is scaled relative to the usual Ekman spin-up timescale. Here  $\zeta_i = \nabla_h^2 \psi_i$  is the vorticity in layer  $i$ , in terms of the stream function  $\psi_i$  with

$$u_i = -\frac{\partial \psi_i}{\partial y} \quad \text{and} \quad v_i = \frac{\partial \psi_i}{\partial x},$$

and  $\Gamma_i$  is the potential vorticity, given in each layer by

$$\Gamma_1 = \zeta_1 - 2F(\psi_1 - \psi_2) = \nabla_h^2 \psi_1 - 2F(\psi_1 - \psi_2)$$

and

$$\Gamma_2 = \zeta_2 + 2F(\psi_1 - \psi_2) = \nabla_h^2 \psi_2 + 2F(\psi_1 - \psi_2).$$

The two evolutionary equations for  $\Gamma_i$  above describe changes in the potential vorticity following each fluid particle, both due to vortex-stretching from 'Ekman-layer suction' and through horizontal viscous diffusion:

Given the values of both  $\Gamma_1$  and  $\Gamma_2$  at any time, obtained from solving the potential vorticity equations, the corresponding values of the stream function can be obtained by subtracting the definitions above for  $\Gamma_1$  and  $\Gamma_2$  to give an elliptic equation for  $(\psi_1 - \psi_2)$ . Solving this gives the value of  $(\psi_1 - \psi_2)$  everywhere, which can then be substituted into, say, the definition for  $\Gamma_1$  to give a Poisson equation for  $\psi_1$ . Having solved for  $(\psi_1 - \psi_2)$  and  $\psi_1$  everywhere, the values of  $\psi_2$  follow immediately.

Note that this formulation accounts for a scaled interface displacement of  $\eta = \frac{1}{2} Ro F d (\psi_1 - \psi_2)$ , when displacements due to rotation effects are relatively small, which is valid provided  $\Delta\rho^*/\rho^* \ll Ro \ll 1$ .

The boundary conditions on the flow are that the stream function in each layer matches onto the appropriate uniform flow at infinity, so that  $\psi_i \sim -U_i y$  and  $\zeta_i \rightarrow 0$  as  $r \rightarrow \infty$ , and that both  $\psi_i$  and  $\partial\psi_i/\partial r$  are zero on  $r = 1$ .

## NUMERICAL METHOD

As described in detail in Blanchonette (1995), the numerical technique used in this study is based on centred finite-difference approximations to the equations above on a conformally-transformed and stretched spatial grid. The parabolic equations for the potential vorticity  $\Gamma_i$  in each layer were solved using a ADI approach, with iterative correction of the velocities in the advective terms at each time step. The coupled elliptic equations for  $\psi_i$  were solved using the 'mgd9v' multigrid routine described in de Zeeuw, (1990). The no-slip boundary conditions on the cylinder were implemented through a boundary condition on the vorticity, using a similar method to that used by Becker (1991), which is in turn was based upon a modified form of that in Israeli (1972).

## RESULTS

As an illustration of the overall flow in both layers, plots of the vorticity  $\zeta$  and stream function  $\psi$  are shown in Figure 2 for  $F = 0$  and when the scaled velocities of the upper and lower layers are  $U_1 = 0.2$  and  $U_2 = 1.8$  respectively. As for the equivalent one-layer flow, it is the effective value of  $\lambda$  in each layer, namely  $\lambda U_i$ , which determines whether separation occurs, although clearly the slower layer is partly 'driven' by an interaction with the faster layer, through the 'Ekman-layer suction' terms in the potential vorticity equations. This is most evident in lower-layer stream function plots shown in Figure 2, where there is a large separated region beneath the region where the upper-layer boundary layer has separated from the cylinder (as evidenced by the vorticity  $\zeta_2$ ). If there was no interaction between the layers then we would expect the separated region in the lower layer to be significantly smaller, based on  $\lambda U_1 = 0.8$  being only slightly greater than the critical value of 0.5 for separation to occur in a single-layer model.

Of particular interest in an analysis of the numerical results is the variation in the location of the separation point as a function of  $\lambda$  for various vertical shears. Prior to this, however, we need to decide how to define the separation point in the context of the numerical calculations because the classical definition, namely the point where the flow direction near the surface reverses (and tangential shear stress vanishes), is not necessarily the most appropriate choice when the boundary-layer thickness  $\delta$  is nonzero.

An alternative definition of the separation point, based partly on Smith's (1985) analysis of the non-rotating flow, is that it is the position where the tangential pressure gradient changes sign. This definition also has a geometrical interpretation because for a stationary surface it is the point where the normal vorticity gradient vanishes, as would occur when a separating boundary layer leaves tangentially from the surface of the cylinder.



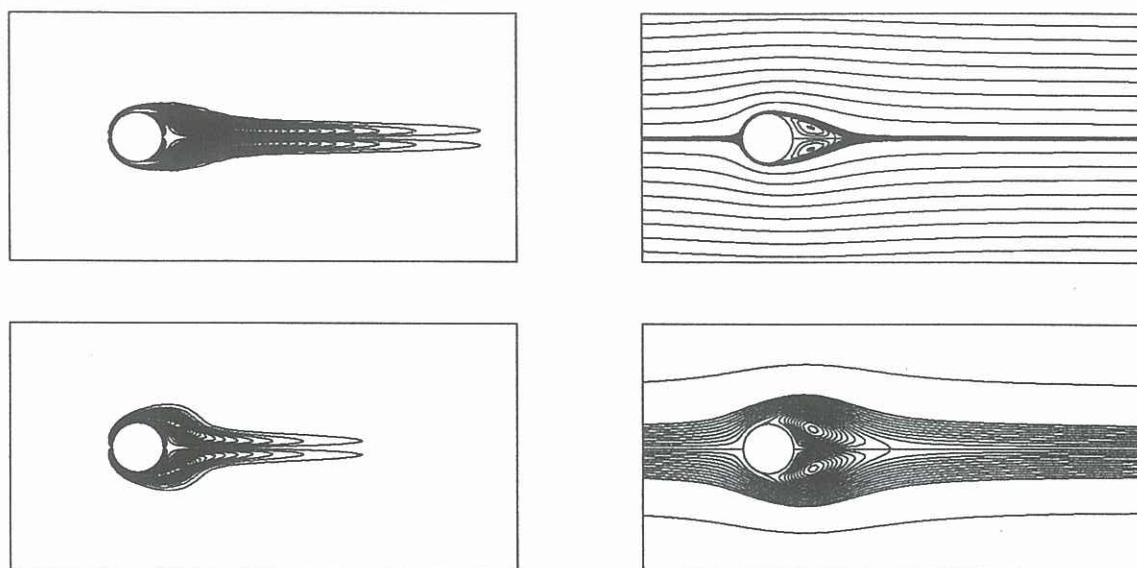


Figure 2 Contour plots of the vorticity  $\zeta$  (left) and streamfunction  $\psi$  (right) in the upper and lower layers for  $\lambda = 4$ ,  $\delta = 0.14$  and  $F = 0$ , when  $U_1 = 0.2$  and  $U_2 = 1.8$ .

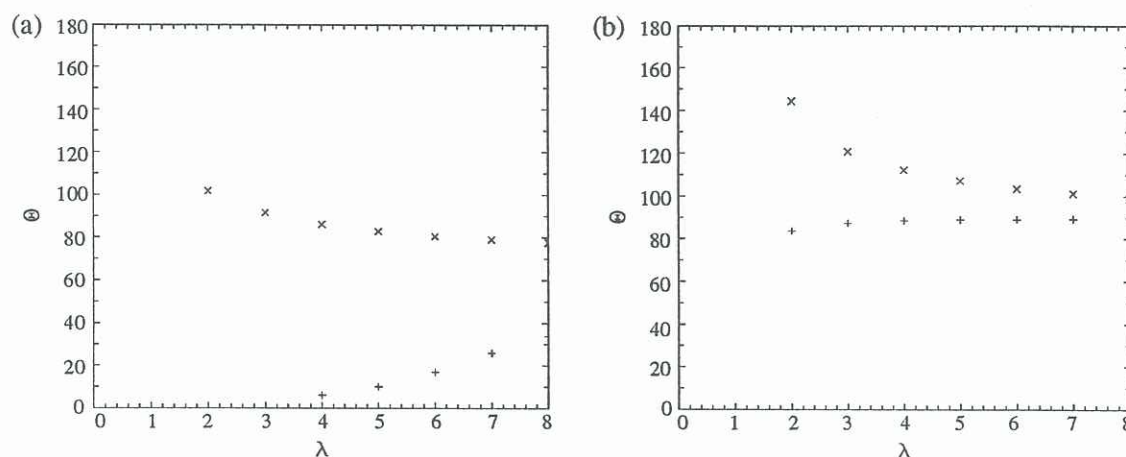


Figure 3 The location of the separation point in the upper (x) and (+) lower layers as a function of  $\lambda$  using (a) the pressure-gradient definition (b) the classical shear-stress definition.

To illustrate the difference in the location of the separation point according to these two definitions, Figure 3 shows their variation in each layer for various values of  $\lambda$ , obtained from the numerical calculations of Blanchonette (1995) using the same shear velocities and boundary-layer thickness as in Figure 2. Clearly, the two points do not coincide at finite Reynolds numbers  $\lambda/\delta^2$ , although it could be argued that they appear to approach each other as  $\lambda$  increases, which is consistent with their coincidence for a non-rotating flow as  $Re \rightarrow \infty$ .

Note that neither of these definitions of the separation point necessarily correspond with that used by Brevdo & Merkin, who identified the separation point as the position where their numerical calculations for the boundary-layer flow 'break down' when they are solved by marching around the cylinder from the forward stagnation point. In fact, this breakdown only occurs because the specified tangential pressure gradient in the boundary-layer calculations does not allow for the

distortion of the outer inviscid flow by the separating boundary layer, so their 'separation point' does not necessarily relate in any way to the place where the boundary-layer flow actually separates. In a non-rotating flow, for example, these points are in different locations.

In a one-layer rotating flow the separation of the boundary layer is not necessarily accompanied by a region of reversed flow (Becker, 1991), but it is also true that reversed flow in the boundary layer does not necessarily imply that separation has occurred. For example, Brevdo & Merkin demonstrate that when  $(U_2 - U_1) > \sqrt{2}$  the boundary layer in the lower layer has reversed flow adjacent to the cylinder, even for  $\lambda = 0$  when the usual type of separation would not occur. This example clearly emphasizes the difference between *separation* and the presence of *reversed flow* in the boundary layer. In this problem, separation tends to be driven by the flow in the layer with the larger far-field velocity  $U_1$ , and hence the larger effective value of  $\lambda$ .

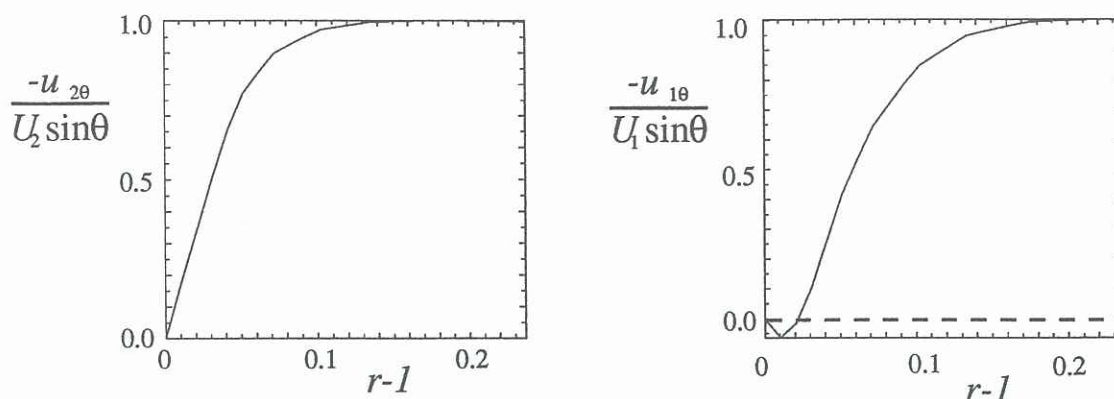


Figure 4 Tangential velocity profiles near the cylinder in each layer, plotted at  $120^\circ$  from the forward stagnation point, for  $U_1 = 0.2$ ,  $U_2 = 1.8$  when  $\lambda = 0.7$ ,  $\delta = 0.03$  and  $F = 0$ .

Despite the limitations of the method used by Brevdo & Merkin when the flow has separated, and also that the numerical calculations of Blanchonette (1995) were performed for a small but finite boundary-layer thickness  $\delta$  rather than in the limit as  $\delta \rightarrow 0$ , the numerical results from both studies are surprisingly similar under some circumstances. As an illustration of this, the tangential velocity profiles at an angle of  $120^\circ$  from the forward stagnation point in each layer are shown in Figure 4 here, corresponding to plots in Figure 8 in Brevdo & Merkin. At this position the upper-layer flow is still attached and it is likely that the small region of reversed flow in the lower layer would have a relatively small effect on the calculations for the much faster upper layer. Also, the separation of the flow in the upper layer would not be expected until further around the cylinder and hence there would probably be only a small distortion of the outer flow, so that Brevdo & Merkin's assumed potential flow forcing may be reasonably accurate in this case.

## DISCUSSION

Despite some similarities between the boundary-layer flow described by Brevdo & Merkin (1985) and that in the numerical results both here and in Blanchonette (1995), the former are inappropriate once the flow in the upper layer has separated because they are based on an incorrect boundary-layer forcing.

Blanchonette (1995) has demonstrated that many of the features of the flows here are also apparent for a non-zero Froude numbers, although in that case the slope in the interface between the layers introduces some additional effects which are related to one-layer flow on a  $\beta$  plane.

Foster (1989) examined a related flow in a linearly stratified fluid, for which the cylinder does not extend throughout the full depth of the fluid, and he notes that the  $Ro F/E^{1/2}$  is an important parameter combination in that case. In a future study the effect of this parameter will be examined for low-Rossby number rotating flow past a cylinder in a linearly-stratified fluid.

## REFERENCES

- Barcion, V., 1970, "Some inertial modifications of the linear viscous theory of steady rotating fluid flows", *Physics of Fluids*, Vol. 13, pp. 537-544.
- Becker, A., 1991, "The separated flow past a cylinder in a rotating frame", *J. Fluid Mech.*, Vol. 224, pp. 117-132.
- Blanchonette, P., 1995 "Flow past a cylinder in a rotating frame", Ph.D. thesis, Monash University.
- Boyer, D.L., 1970, "Flow past a circular cylinder in a rotating frame", *Trans ASME D: J. Bas. Eng.*, Vol. 92, pp. 430-436.
- Boyer, D.L. & Davies, P.A., 1982, "Flow past a circular cylinder on a  $\beta$  plane", *Phil. Trans. Roy. Soc. Lond. A*, Vol. 306, pp. 533-556.
- Brevdo, L. & Merkin, L., 1985, "Boundary-layer separation of a two-layer rotating flow on an  $f$  plane", *Proc. Roy. Soc. Lond. A*, Vol. 400, pp. 75-95.
- de Zeeuw, P.M., 1990, "Matrix-dependent prolongation and restrictions in a blackbox multi-grid solver", *J. Comp. Appl. Math.*, Vol. 33, pp. 1-27.
- Foster, M.R., 1989, "Rotating stratified flow past a steep-sided obstacle: incipient separation", *J. Fluid Mech.*, Vol. 206, pp. 47-73.
- Gill, A.E., 1982, "Atmosphere-Ocean Dynamics", Academic, New York.
- Israeli, M., 1972, "On the evaluation of iteration parameters for the boundary vorticity", *Stud. Appl. Math.*, Vol. 51, pp. 67-71.
- Matsuura, T. & Yamagata, T., 1986, "A numerical study of a viscous flow past a circular cylinder on an  $f$  plane", *J. Met. Soc. Japan*, Vol. 63, pp. 151-166.
- Merkin, L. & Solan, A., 1979, "The separation of flow past a cylinder in a rotating system", *J. Fluid Mech.*, Vol. 92, pp. 381-391.
- Page, M.A., 1987, "Separation and free-streamline flows in a rotating fluid at low Rossby number", *J. Fluid Mech.*, Vol. 179, pp. 155-177.
- Page, M.A. & Duck, P.W., 1993, "The structure of the separated flow past a circular cylinder in a rotating fluid", *Geophys. Astrophys. Fluid Dyn.*, Vol. 58, pp. 197-223.
- Smith, F.T., 1985, "The structure for laminar flow past a bluff body at high Reynolds number", *J. Fluid Mech.*, Vol. 155, pp. 175-191.
- Walker, J.D. & Stewartson, K., 1972, "The flow past a circular cylinder in a rotating frame", *Z. angew. Math. Phys.*, Vol. 23, pp. 745-752.